EVS38
Göteborg, Sweden, June 15-18, 2025

Characterization of High-Energy Prismatic NMC (631) Cells: A Combined Incremental Capacity and Electrochemical Impedance Spectroscopy Approach

Kashif Raza[1], Maitane Berecibar [1], Md Sazzad Hosen [1*]
[1]*MOBI-Electromobility Research Centre, Department of Electrical and Energy Technology, Vrije Universiteit Brussel, Pleinlaan 2, 1050 Brussels, Belgium.*
[*]*Correspondance: md.sazzad.hosen@vub.be*

Executive Summary

Electric vehicles are becoming more common daily because countries are moving towards net-zero emissions. Different generations of NMC battery cells are used for EV applications. This paper performs incremental capacity analysis (ICA) and electrochemical impedance spectroscopy (EIS) analysis of NMC(631) generation battery cells at 3 different temperatures and different cyclic conditions. At high temperatures, there is a significant increase in impedance at all frequency ranges, and a shift in the peaks of the ICA is observed. Cells cycled at elevated temperature (45°C) experienced catastrophic capacity loss, dropping to as low as 34% of their original capacity within the completion of 700 full equivalent cycles (FECs). In stark contrast, cells operated within a moderate state-of-charge window (20-80%) at lower temperatures (5°C and 25°C) maintained over 97% of their original capacity throughout the same cycling period.

1 Introduction

Lithium-ion batteries (LIBs) are the cornerstone of modern energy storage, powering applications from consumer electronics to electric vehicles (EVs). Among LIB cathodes, lithium nickel manganese cobalt oxides (NMC) stand out for their well-rounded performance. In fact, NMC-based cells are used by most EV manufacturers due to their high energy density, adequate power capability, and long-term stability [1,2]. Recently, nickel-rich NMC formulations (Ni content ≥60%) have gained attention as next-generation cathodes because they deliver high specific capacity at reduced cobalt content. One such composition is NMC (631), which contains roughly half the cobalt of the earlier NMC (622), NMC (532) chemistry, while still achieving excellent capacity and thermal stability. This makes NMC (631) a promising candidate for lowering cost and improving sustainability without sacrificing performance [3]. Understanding how batteries perform at different operating temperatures is essential for maintaining efficiency and durability.

Operating temperature is a critical factor influencing battery performance and longevity. At low temperatures (e.g., around 0–5 °C), cell kinetics slow dramatically – ion diffusion and charge-transfer reactions are hindered, leading to higher internal resistance and a marked drop in usable capacity [4,5]. Conversely, elevating the temperature tends to improve immediate performance (by accelerating electrochemical kinetics), but this comes at the cost of hastened side reactions and degradation. High operating temperatures significantly accelerate aging mechanisms like solid electrolyte interphase(SEI) growth and loss of active material [6], resulting in permanent capacity loss over time. Maintaining cells within an optimal temperature window is therefore essential to balance efficiency and durability.

To rigorously evaluate cell behavior under different thermal conditions, one must employ diagnostic techniques that probe beyond simple capacity measurements. Incremental Capacity Analysis (ICA) is one such powerful tool, by examining the differential capacity curve. ICA, a prominent technique in battery modeling, is utilized

for State-of-Health (SoH) estimation, Remaining Useful Life (RUL) prediction, and degradation mode identification [7–10]. ICA and its inverse technique, differential voltage analysis (DVA) were first introduced by [11] as a first non-technique for diagnosis from laboratory testing data. One of the shortcomings of ICA is that the positive and negative electrode responses are convoluted. Complementarily, Electrochemical Impedance Spectroscopy (EIS) is a powerful non-invasive method for SoH estimation and tracking degradation behaviors over time [12]. ICA can reveal subtle shifts in the voltage profile associated with phase transitions or aging-related changes inside the cell. This technique has grown in popularity because it effectively identifies specific battery degradation modes non-invasively, acting as a fingerprint of the cell's internal state-of-health [13]. Likewise, EIS provides complementary insight by measuring the cell's impedance across a spectrum of frequencies. EIS is a widely used non-destructive method that characterizes the kinetics of electrochemical processes in a battery, allowing one to distinguish contributions from bulk resistances, charge-transfer reactions, and diffusion phenomena. Together, ICA and EIS offer a comprehensive diagnostic framework – the former sensitively tracks changes in the capacity–voltage signature, and the latter quantifies internal resistive and transport properties, which are invaluable for understanding how and why battery performance shifts under different temperatures. Incremental capacity is calculated by using the following equation (*1*).

$$IC = \frac{dQ}{dV} \cong \frac{\Delta Q}{\Delta V} \tag{1}$$

High-energy cells are commonly used for PHEV and EV applications. This study investigates the high-energy NMC 75 Ah capacity cells through ICA analysis and EIS analysis at different temperatures. This study seeks to fill that gap by systematically characterizing the performance of NMC (631) prismatic cells under three representative temperatures: 5 °C (cold), 25 °C (ambient), and 45 °C (hot). Using a standardized 1C charge and 1C discharge protocol, we capture the cell's behavior under realistic operating conditions across cold, moderate, and elevated temperatures. We then apply ICA and EIS diagnostics to these cycling tests, correlating temperature-induced changes in the incremental capacity curves and impedance spectra with underlying physical changes in the cell. This combined approach provides a multi-faceted view of NMC631's performance envelope, yielding new data and insights. The results offer valuable guidance for battery scientists and engineers working on high-energy lithium-ion cells, supporting the development of robust battery systems that can maintain reliability from winter cold to summer heat.
The rest of the paper includes the experimental setup details in Section 2. Section 3 discusses the results, which starts with first ICA and then EIS analysis. Section 4 discusses the conclusion.

2. Experimental Setup

The specifications of the cells are in Table 1. It includes six cells tested under various conditions, with two cells per condition. Figure 1 illustrates the testing workflow and sample cell specifications. Three conditions are selected under which batteries are tested. For each condition, 2 cells are tested to prove the repeatability of the experiment. In the characterization of the cells after completing the 100 full equivalent cycles (FECs), the capacity test and OCV test are performed at C/3-rate at the cycling temperature. Before performing EIS, cells undergo the capacity test at 25°C to check the capacity value under stable conditions, and then EIS is performed at 25°C. Thermal chambers are used to keep the ambient temperature constant. The preliminary findings compare the cells' Beginning-of-Life (BoL) performance with their state after 100 Full Equivalent Cycles (100 FEC).

Table 1. Li-ion battery cell specifications

Battery Chemistry	NMC
Capacity [Ah]	75
Nominal Voltage [V]	3.72
Voltage Range [V]	2.8 – 4.35
Energy Density – Weight [Wh/kg]	220
Energy Density – Volume [Wh/L]	505

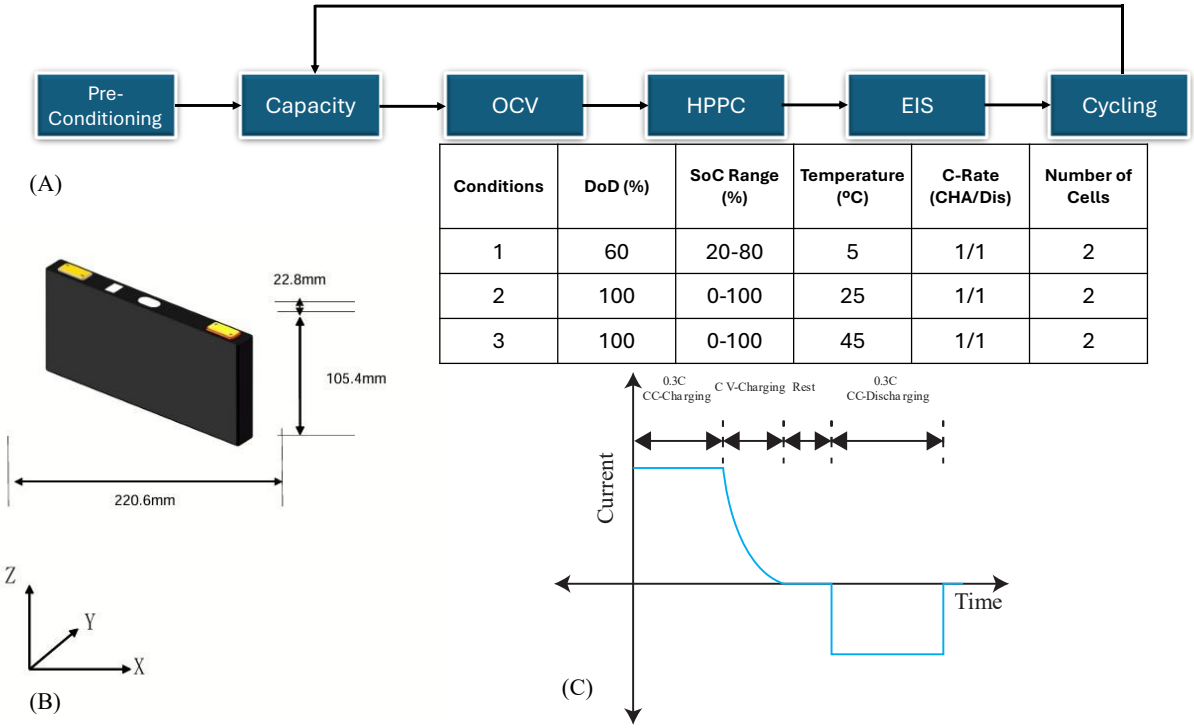

Conditions	DoD (%)	SoC Range (%)	Temperature (°C)	C-Rate (CHA/Dis)	Number of Cells
1	60	20-80	5	1/1	2
2	100	0-100	25	1/1	2
3	100	0-100	45	1/1	2

Figure 1. High-energy cells overview diagram (a). The flow of reference performance test and cycling under the conditions in these cells is tested (b). dimensions and 3D view of the sample cell (C). Sample capacity test section (1 cycle).

3 Results

3.1 ICA Analysis

The ICA results in Figure 2 illustrate the dQ/dV (change in charge over the change in voltage) curves across a voltage range for various operating temperatures. Each cell underwent cycling up to 600 or 700 FECs, providing detailed insights into their SoH evolution. The ICA peaks represent key electrochemical reactions and changes in battery behavior with cycling, allowing for insights into capacity fading and resistance growth over time.

For cells N01 and N02, under 5°C cycling, ICA curves remain relatively consistent throughout cycling, maintaining clear and sharp peak definitions around 3600–3800 mV, indicating stable phase transition behavior with minor degradation. Corresponding SoH data for the cells is in Table *2*. Both cells maintain more than 98% SoH after 700 FECs. This stability suggests minimal structural degradation and electrolyte-side reactions within this cycling regime and operating conditions. This exceptional performance stems from their battery-friendly operating parameters. The limited depth of discharge (60%) significantly reduces mechanical stress on electrode materials by avoiding complete discharge cycles. Equally important, their moderate SoC range (20-80%) strategically avoids both extremes where accelerated degradation typically occurs.

Table 2. Last SoH for the cells after cycling up to 700.

Conditions	Cell No.	SoH (%)
Condition I	N01	98.88
	N02	98.25
Condition II	N03	98.62
	N04	97.7
Condition III	N05	61.6
	N06	34.08

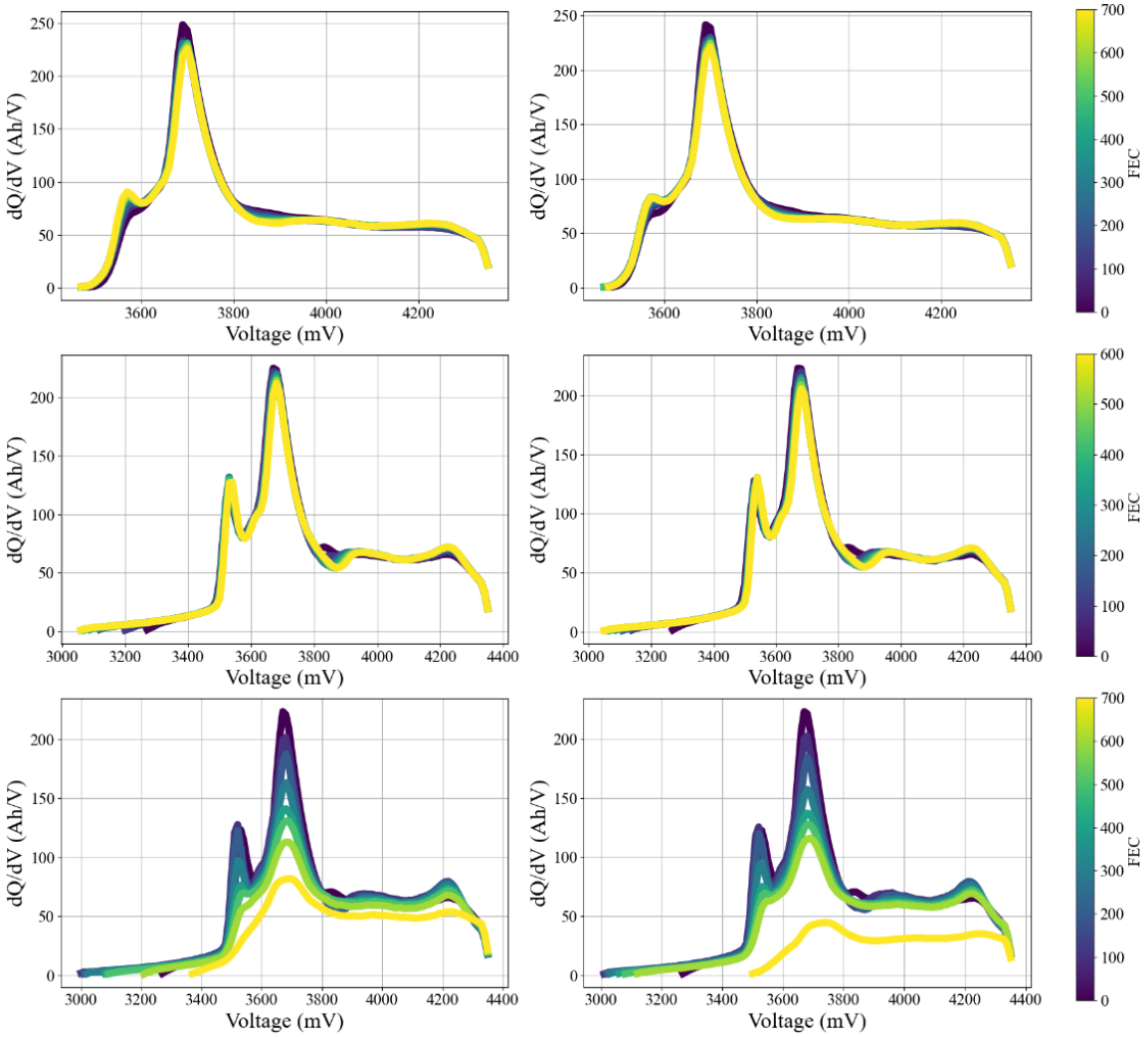

Figure 2. ICA results for 6 cells under testing. For each condition, 2 cells are tested (A). & (B). cells at 5°C, (C). & (D). cells at 25°C and (E). & (F). cells at 45°C

Cells N03 and N04, operating under Condition II, exhibited good but slightly reduced performance compared to the first pair, maintaining SoH values above 97%. These cells experienced full depth of discharge (100%) cycling, which necessarily imposes greater volume changes and mechanical stress on electrode materials during each charge-discharge cycle. Their exposure to the complete SoC range (0-100%) meant these cells regularly operated in the high and low extremes where various degradation mechanisms accelerate. The room temperature condition (25°C) represents a moderate thermal environment but still allows degradation reactions to proceed faster than in the cooler Condition 1 cells. The distinctive dual-peak pattern in their ICA curves remained relatively stable throughout cycling. One of the key differences in the evolution of the peaks for both cells is that peak 1, before 3.6V for the cells at condition I, is less sharp compared to the cells at 25°C. ICA curve for the cell under condition I after 3.8V, the curve is flatter compared to the cell at 25°C, which has a clear valley and peak.

Cells N49 and N50, subjected to Condition III, experienced dramatic capacity loss, with SoH values plummeting to 61.6% and 34.08%, respectively. The combination of full depth of discharge cycling, complete SoC range utilization, and most critically, elevated temperature (45°C), created ideal conditions for accelerated degradation. High temperature acts as a catalyst for numerous degradation mechanisms: it speeds up SEI layer growth on the anode, accelerates electrolyte decomposition reactions, enhances transition metal dissolution from cathode materials, increases gas generation within the cell, and potentially damages electrode binders, leading to delamination. These multifaceted degradation processes manifest clearly in their ICA curves, which show substantial peak height reduction, shape changes, and the emergence of new features in the 4000-4200 mV region as cycling progresses. The visible evolution of these curves provides a detailed fingerprint of the ongoing degradation mechanisms.

The significant difference in degradation rates between cells N49 and N50, despite identical testing conditions, highlights an important reality in battery manufacturing—inherent cell-to-cell variability. While both cells experienced catastrophic capacity loss, N50 degraded much more severely than N49. This difference likely stems from microscopic variations in electrode microstructure, small differences in electrolyte composition or quantity, variations in electrode alignment, particle size distribution differences, or minor impurity level variations. The extreme conditions of high-temperature full cycling effectively magnified these small manufacturing differences, resulting in dramatically different lifespans between otherwise identical cells.

3.2 **EIS Analysis**

EIS results for all 6 cells from the beginning of life to 600 or 700 FEC are presented in Figure *3*. The presented data in the figure are the Nyquist curves at 100% SoC. These Nyquist plots display the relationship between the real (x-axis) and imaginary (y-axis) components of impedance across different frequencies, offering insights into various electrochemical processes occurring within the batteries as they age. Figure *3* (A) and (B) represent the EIS results for cells operating under condition I. These cells showed excellent capacity retention in the ICA analysis, and their impedance characteristics confirm this exceptional stability. The Nyquist plots for these cells display minimal changes across the full range of cycling (from BoL to FEC700). The semicircle in the high-frequency region, which typically represents the charge transfer resistance and solid electrolyte interphase (SEI) layer, remains remarkably consistent throughout cycling. This stability indicates that the SEI layer formed on these cells remains thin and stable, without significant growth over hundreds of cycles. The low-frequency tail, representing diffusion processes, also shows minimal changes, suggesting that lithium-ion transport pathways remain largely unobstructed. The slight shifts observed between different cycle counts are orderly and progressive, indicating a gradual and controlled aging process rather than any abrupt degradation mechanisms. This controlled evolution of impedance aligns perfectly with the stable SoH values observed for these cells, confirming that the mild operating conditions (moderate SoC range and low temperature) successfully preserve the electrochemical properties of the cell components.

Figure *3* (C) and (D) represent the EIS results for cells operating under condition II. While these cells also maintained good SoH, their impedance changes are also stable. These cells also present stable impedance spectra with slight increases in charge transfer resistance observed at higher FECs. This minor resistance rise aligns well with the marginally reduced SoH and stable ICA patterns, reflecting robust electrochemical and structural stability. The mid-to-low frequency region also shows more pronounced changes compared to Condition I cells, with a visible separation between earlier and later cycles. This separation indicates that full cycling at room temperature is gradually altering the bulk properties of the electrodes, affecting lithium-ion diffusion pathways. However, these changes occur in a relatively consistent manner without the appearance of new features that would indicate severe degradation mechanisms.

Figure *3* (E) and (F) represent the EIS results for cells operating under condition III at 45°C. The EIS data for these cells reveals dramatic changes that correlate with their severe capacity loss observed in the ICA analysis. The key observation is the substantial growth of impedance across all frequency regions. There is a significant shift observed in the Nyquist curve, which indicates an increase in ohmic resistance, which is the combination of contact resistance and electrolyte. The semi-circle region is also growing dramatically, which represents the increase in charge transfer resistance. In the later cycles at 600 and 700 FEC, there are indications of two semi-circle regions where the first one shows the SEI layer growth, and then the second is an increase in charge transfer resistance. Furthermore, the low-frequency region also shows significant changes, with the curves extending much further along both axes compared to the other conditions. This extension indicates severely compromised lithium-ion diffusion pathways, likely due to structural degradation within the electrodes, and gas formation blocking ion transport channels. Most notably, the 700 FEC measurements (gray markers) in Figure 3 (F) for the N06 cell show dramatically different behavior compared to earlier cycles, which is also observed in the ICA analysis and its SoH value of 34%.

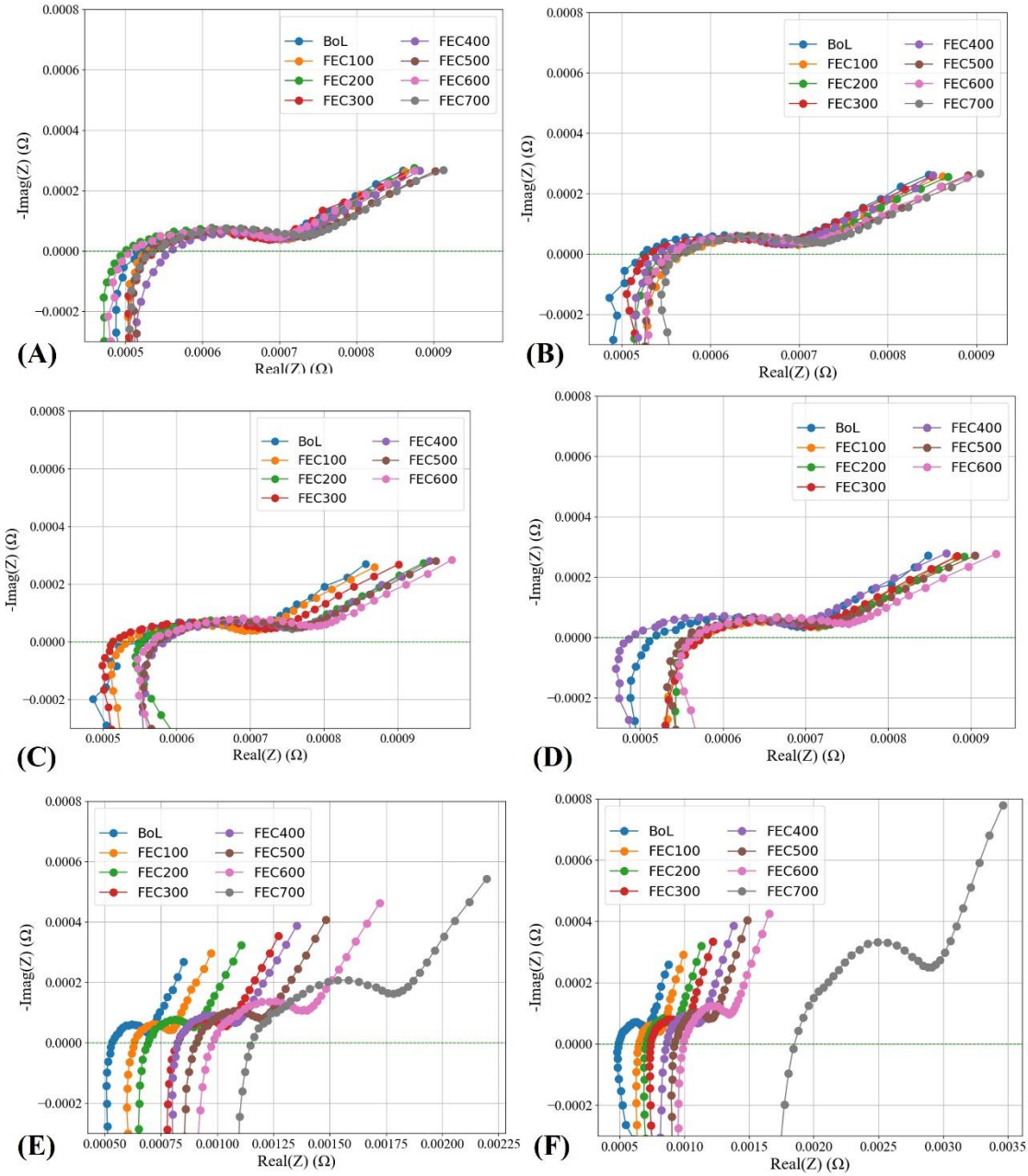

Figure 3. Nyquist plot for six cells after some hundreds of cycling (A). & (B). Cells are at 5°C, (C). & (D). Cells are at 25°C and (E). & (F). Cells are at 45°C

This integrated ICA and EIS analyses clearly illustrate variability in the electrochemical robustness of NMC (631) prismatic cells under study. Cells N01, N02, N03, and N04 demonstrate excellent stability and minor degradation even after prolonged cycling, signifying effective electrochemical management. Conversely, cells N49 and N50 reveal significant susceptibility to severe electrochemical and structural degradation, highlighting the critical need for optimized electrolyte formulations, improved thermal management, and stringent manufacturing controls. These results provide essential insights into longevity, reliability, and optimal design considerations for advanced lithium-ion battery cells.

4. Conclusion

This comprehensive analysis of both ICA and EIS data provides deep insights into battery degradation under different operating conditions. The combined results clearly demonstrate that battery longevity is dramatically influenced by operating parameters, with temperature emerging as the most critical factor, followed by depth of discharge. Furthermore, the clear correlation between ICA features and EIS characteristics suggests that combining these complementary diagnostic techniques could enable more precise early detection of degradation mechanisms, potentially allowing for adaptive management strategies that adjust operating parameters as

batteries age to maximize their useful life.

Acknowledgments

The authors gratefully acknowledge the project NEMO, which has received funding from the European Union's Horizon Europe research and innovation program under grant agreement No 101069756.

References

[1] Salgado RM, Danzi F, Oliveira JE, El-Azab A, Camanho PP, Braga MH. The latest trends in electric vehicles batteries. Molecules 2021;26:1–41. https://doi.org/10.3390/molecules26113188.

[2] Gorsch J, Schneiders J, Frieges M, Kisseler N, Klohs D, Heimes H, et al. Contrasting a BYD Blade prismatic cell and Tesla 4680 cylindrical cell with a teardown analysis of design and performance. Cell Rep Phys Sci 2025;6. https://doi.org/10.1016/j.xcrp.2025.102453.

[3] Zhang N, Li J, Li H, Liu A, Huang Q, Ma L, et al. Structural, Electrochemical, and Thermal Properties of Nickel-Rich LiNi x Mn y Co z O 2 Materials. Chemistry of Materials 2018;30:8852–60. https://doi.org/10.1021/acs.chemmater.8b03827.

[4] Luo H, Wang Y, Feng YH, Fan XY, Han X, Wang PF. Lithium-Ion Batteries under Low-Temperature Environment: Challenges and Prospects. Materials 2022;15:1–28. https://doi.org/10.3390/ma15228166.

[5] Wittman R, Dubarry M, Ivanov S, Juba BW, Romàn-Kustas J, Fresquez A, et al. Characterization of Cycle-Aged Commercial NMC and NCA Lithium-ion Cells: I. Temperature-Dependent Degradation. J Electrochem Soc 2023;170:120538. https://doi.org/10.1149/1945-7111/ad1450.

[6] Madani SS, Shabeer Y, Allard F, Fowler M, Ziebert C, Wang Z, et al. A Comprehensive Review on Lithium-Ion Battery Lifetime Prediction and Aging Mechanism Analysis. Batteries 2025:1–68.

[7] M. Berecibar. 2016 IEEE Vehicle Power and Propulsion Conference (VPPC). IEEE; 2016.

[8] Wu Y, Xue Q, Shen J, Lei Z, Chen Z, Liu Y. State of Health Estimation for Lithium-Ion Batteries Based on Healthy Features and Long Short-Term Memory. IEEE Access 2020;8:28533–47. https://doi.org/10.1109/ACCESS.2020.2972344.

[9] Maures M, Capitaine A, Delétage JY, Vinassa JM, Briat O. Lithium-ion battery SoH estimation based on incremental capacity peak tracking at several current levels for online application. Microelectronics Reliability 2020;114. https://doi.org/10.1016/j.microrel.2020.113798.

[10] Jan Figgener. Degradation mode estimation using reconstructed open circuit voltage curves from multi-year home storage field data 2024.

[11] Bloom I, Jansen AN, Abraham DP, Knuth J, Jones SA, Battaglia VS, et al. Differential voltage analyses of high-power, lithium-ion cells: 1. Technique and application. J Power Sources 2005;139:295–303. https://doi.org/10.1016/J.JPOWSOUR.2004.07.021.

[12] Teliz E, Zinola CF, Díaz V. Identification and quantification of ageing mechanisms in Li-ion batteries by Electrochemical impedance spectroscopy. Electrochim Acta 2022;426. https://doi.org/10.1016/j.electacta.2022.140801.

[13] Dubarry M, Anseán D. Best practices for incremental capacity analysis. Front Energy Res 2022;10:1–18. https://doi.org/10.3389/fenrg.2022.1023555.

Presenter Biography

Kashif Raza is a Ph.D. student at Vrije Universiteit Brussels (VUB). He received a bachelor's degree in Electrical Engineering from the University of Gujrat and a master's from Information Technology University (ITU) Lahore. After completing his master's degree in 2021, he worked as a research assistant on Li-ion batteries research at Lahore University of Management Sciences (LUMS). His research interests are data-driven modeling, energy storage, and battery algorithm development.